



10 **Abstract**

11 We examine the impacts of atmospheric aerosols on Arctic and global climate  
12 using a series of 20<sup>th</sup> century transient simulations from Community Climate System  
13 Model version 4 (CCSM4). We focus on the response of surface air temperature to the  
14 direct radiative forcing driven by changes in sulfate and black carbon (BC)  
15 concentrations from 1975 to 2005 and we also examine the response to changes in  
16 sulfate, BC, and organic carbon (OC) aerosols collectively. The direct forcing from  
17 sulfate dominates the aerosol climate effect. Globally averaged, changes in all three  
18 aerosols produce a cooling trend of 0.015 K/decade during the period 1975-2005. In the  
19 Arctic, surface air temperature has large spatial variations in response to changes in  
20 aerosol concentrations. Over the European Arctic, aerosols induce about 0.6 K/decade  
21 warming which is about 1.8 K warming over the 30 years period. This warming is  
22 triggered mainly by the reduction in sulfate and BC emissions over Europe since the  
23 1970s and is reinforced by sea ice loss and a strengthening in atmospheric northward heat  
24 transport. Changes in sulfate concentrations account for about two thirds of the warming  
25 and BC for the remaining one-third. Over the Siberian and North American Arctic,  
26 surface air temperature is likely influenced by changes in aerosol concentrations over  
27 Asia. An increase in sulfate optical depth over Asia induces a large cooling while an  
28 increase in BC over Asia causes a significant warming.

## 29 **1. Introduction**

30 The Arctic (the region poleward of 60°N) has warmed dramatically since the  
31 1970s, by ~1.5°C. The warming in the Arctic is at least two times larger than the global  
32 mean temperature increase [e.g., Serreze et al., 2009]. This phenomenon is known as  
33 Arctic amplification [e.g., Manabe and Stouffer, 1980]. The detailed mechanisms causing  
34 the warming are not fully understood [Serreze and Barry, 2011]. Climate model  
35 simulations have shown that ice-albedo feedback is likely to account for much of the  
36 Arctic warming [e.g., Holland and Bitz, 2003; Screen and Simmonds, 2010], whereby  
37 warmer temperatures cause highly reflective snow and sea ice to melt, decreasing the  
38 Earth's planetary albedo and thus inducing further warming. The lapse rate feedback may  
39 be equally important [Armour et al., 2013; Pitham and Mauritzen, 2013].

40 While the feedbacks triggered by greenhouse gas warming may dominate Arctic  
41 warming, short-lived aerosols in the atmosphere also are an important forcing agent in  
42 this region [e.g., Quinn et al., 2008; Koch et al., 2009; Shindell and Faluvegi, 2009;  
43 Serreze and Barry, 2011]. Further, climate changes triggered by aerosol trends will also  
44 be enhanced by local feedbacks and modified by circulation changes. Shindell and  
45 Faluvegi [2009] conducted sensitivity experiments using the GISS-ER climate model and  
46 suggested that decreasing concentrations of sulfate aerosols and increasing concentrations  
47 of BC have substantially contributed to Arctic warming over the last three decades. They  
48 also found Arctic temperature changes depend on the location of BC in the atmosphere.  
49 Increasing concentrations of BC in low/mid-latitude causes warming in the Arctic, while  
50 increasing BC in the Arctic itself causes cooling in the Arctic. In another climate model  
51 study, Sand et al. [2013] produced similar results to Shindell and Faluvegi [2009] and

52 attributed the response in Arctic surface air temperature mainly to the changes in  
53 atmospheric northward heat transport (NHT). Increasing atmospheric BC in the Arctic  
54 leads to a weakening of NHT and thus surface cooling; when BC is located in mid-  
55 latitudes, NHT is strengthened leading to Arctic surface warming. Arctic surface  
56 temperature is also found to be sensitive to the vertical distribution of BC in the CCSM4  
57 [Flanner, 2013]: a layer of BC centered in the upper troposphere produces surface  
58 cooling, while a layer of BC in the lower troposphere causes weak surface warming.  
59 While there has been much focus on the role of BC in Arctic climate, we are interested in  
60 how Arctic climate has been affected by changes in both sulfate and BC aerosol  
61 distributions over the past three decades. As shown below trends in the two are not  
62 homogenous in either space or time.

63 Here, the response of Arctic and global surface air temperature to the trends of  
64 atmospheric sulfate and BC aerosols are examined using 20<sup>th</sup> century simulations from  
65 CCSM4. We performed single forcing experiments, in which only direct radiative forcing  
66 from sulfate aerosols or BC was included. This enables us to isolate the effects of sulfate  
67 and BC and their contributions to the effect of all aerosols on climate. We also examine  
68 the response to changes in sulfate, BC, and OC aerosols collectively. In addition to  
69 surface air temperature, we investigate the response of sea level pressure, sea ice  
70 coverage, cloud radiative forcing and atmospheric NHT to determine the mechanisms  
71 that cause the surface air temperature change in the Arctic during the period 1975-2005.

72

## 73 **2. Model and Experiments**

74 We use CCSM4 with fully-coupled atmosphere, ocean, land and sea ice  
75 components [Gent et al., 2011]. The atmosphere component is the Community  
76 Atmosphere Model 4 (CAM4) [Neale et al., 2011] with a horizontal resolution of  
77  $0.9^\circ \times 1.25^\circ$ . The atmospheric aerosol concentrations were derived from an off-line CAM-  
78 Chem [Lamarque et al., 2012] driven by observationally based estimates of aerosol  
79 emissions [Lamarque et al., 2010; 2011]. Anthropogenic emissions of sulfur species are  
80 an update of Smith et al. [2001; 2004]. The oceanic DMS emission was estimated from  
81 Kettle et al. [1999]. Volcanic and biomass sources of sulfur are excluded [Neale et al.,  
82 2011]. Emissions of BC and OC represent an update of Bond et al. (2007) and Junker and  
83 Liou (2008). The Mie calculations for sulfate assume that it is comprised of  
84 ammonium sulfate with a log-normal size distribution [Neale et al., 2011]. BC and OC  
85 are assumed to age from hydrophobic to hydrophilic at an e-folding time of 1.2 days. The  
86 optics for BC and OC are identical to the optics for soot and water-soluble aerosols in the  
87 Optical Properties of Aerosols and Clouds (OPAC) data set [Hess et al., 1998; Neale et  
88 al., 2011]. Total aerosol optical depth comparisons with AERONET observations indicate  
89 a reasonably good simulation [Lamarque et al. 2010]. Shindell et al. [2013] used this  
90 atmospheric aerosol concentration dataset and demonstrated that it captures total aerosol  
91 optical depth trends of 1980-2000 well over the areas of high aerosol emissions (e.g.,  
92 Europe, eastern North America and south and east Asia), compared with Advanced Very  
93 High Resolution Radiometer (AVHRR) observations. Compared with high-latitude  
94 aircraft campaigns, simulated BC concentrations, using the same emission sources as  
95 Lamarque et al. [2010] but with a previous version of CAM, are within the observed  
96 standard deviation [Koch et al., 2009]. CAM4 includes the direct and semi-direct effects

97 of aerosols, but the aerosol first indirect effect [Twomey et al. 1984] is not included. The  
98 same model and 20<sup>th</sup> century forcing datasets were used for the Coupled Model  
99 Intercomparison Project phase 5 (CMIP5) [Taylor et al., 2012] contributions from  
100 CCSM4.

101 Table 1 lists the details of our individual model experiments. The all-aerosol  
102 simulations were realized by varying the time- and space-evolving mass concentrations  
103 of sulfate, BC and OC aerosols simultaneously. All other forcings were kept fixed at  
104 1850 levels, including surface depositions of BC on snow and sea ice. Three ensemble  
105 members of all-aerosol simulations were obtained from CMIP5 [Meehl et al., 2012]. The  
106 sulfate-only and BC-only single forcing experiments are analogous to the all-aerosol  
107 experiment except for only varying the mass concentrations of sulfate or BC,  
108 respectively. For each experiment, six branch runs were carried out from year 1920 and  
109 run to year 2005, making six ensemble members in each experiment. The restart files of  
110 year 1920 were obtained from 20<sup>th</sup> century total aerosol forcing only integrations with  
111 CCSM4 for CMIP5 [see Meehl et al., 2012]. In addition to six simulations of sulfate-only  
112 forcing, we also include surface air temperature fields from three runs of CMIP5 sulfate-  
113 only [Meehl et al., 2012]. The 1850 control run was also obtained from CMIP5.

114 Figure 1 shows linear trends in optical depths of sulfate and BC from 1975 to  
115 2005. The results are ensemble means of six integrations. Since the 1970s, sulfate aerosol  
116 optical depth decreased significantly in Europe and North America. However, aerosol  
117 optical depth increased in Southeast of Asia, India and the Pacific Ocean region (Fig. 1a).  
118 Globally, there is a decrease in sulfate aerosol optical depth (not shown). Due to the  
119 emissions reductions in Europe and North America, sulfate optical depth decreased over

120 the Arctic, especially over the Eurasian Arctic (Fig. 1b). Sulfate aerosol is almost  
121 entirely scattering, with a single scattering albedo equal to one in the solar spectrum and a  
122 small fraction of absorption in the near-infrared spectrum. Therefore, it causes a net  
123 radiative cooling at the surface by scattering solar radiation back to space and letting less  
124 solar radiation reach the surface [IPCC, 2007, p160]. The mean surface shortwave  
125 radiative flux change in year 2000 due to sulfate is estimated at  $-0.84 \text{ W/m}^2$  globally and  
126  $-0.22 \text{ W/m}^2$  for the Arctic in CCSM4. These estimates were performed by running CAM4  
127 shortwave radiative transfer code twice with adjusted temperatures at all levels.

128 From 1975 to 2005 there were significant reductions in BC optical depth in  
129 Europe, but over the same period there were significant increases in optical depth in India  
130 and China (Fig. 1c). At the same time, emissions of fossil fuel BC declined in the U.S.  
131 [IPCC, 2007, p163]. Thus, the slight increase in BC optical depth over North America  
132 seen in Fig. 1c is possibly due to the downstream transport from Asia. In contrast, there  
133 was a decline in sulfate optical depth over North America and over all of the Arctic (Fig.  
134 1a and 1b). While global mean sulfate emissions declined, BC emissions increased  
135 [Lamarque et al., 2010]. In the Arctic, BC optical depth shows a negative trend over the  
136 European Arctic but a positive trend over the rest of the Arctic (Fig. 1d). BC is a light-  
137 absorbing aerosol, so it absorbs solar radiation and heats the surrounding air [IPCC, 2007,  
138 p163]. The annual mean instantaneous flux change at the surface due to the direct effect  
139 of atmospheric BC is  $-0.46 \text{ W/m}^2$  over the whole globe and  $-0.14 \text{ W/m}^2$  over the Arctic in  
140 model year 2000 in CCSM4.

141

### 142 **3. Results**

### 143 3.1. Surface air temperature trends

144 Figure 2 depicts the time-evolving surface air temperature response to the change  
145 in all aerosols, sulfate-only and BC-only from 1920 to 2005. The all-aerosol, sulfate-only  
146 and BC-only runs have ensemble members of three, nine and six, respectively (Table 1).  
147 Globally, surface air temperature from all-aerosol forcing shows a significant negative  
148 trend of about 0.02 K/decade 1920-2005 and  $\sim 0.015$  K/decade 1975-2005 in CCSM4.  
149 This result agrees with the study by Fyfe et al. [2013] that other forcing (primarily  
150 aerosol forcing) causes a modest Arctic cooling among CMIP5 models from 1970-2005.  
151 Surface air temperature from sulfate-only forcing resembles that of the all-aerosol  
152 forcing. Therefore, the response of global surface air temperature to all aerosols is  
153 dominated by the direct forcing by sulfate. BC has a warming effect on global  
154 temperature ( $\sim 0.1$  K), but this is almost completely offset by the cooling influence from  
155 organic carbon, which is co-emitted with BC [e.g., Bond et al., 2013]. In the Arctic,  
156 surface air temperature is more variable, with no clear trends in Arctic-averaged surface  
157 air temperature from 1975 to 2005 in any of the three cases. The BC-only case indicates  
158 some warming from 1980 to 2000, followed by a cooling 2000-2010, but this is not  
159 statistically significant. However, there are statistically significant positive and negative  
160 temperature trends in different regions of the Arctic, which in this Arctic-wide average  
161 offset each other.

162 Geographic distributions of surface air temperature trends 1975-2000 are shown  
163 in Figure 3. We focus primarily on the changes in the Arctic, but show the global maps to  
164 aid interpretation of what is driving the Arctic changes. Direct radiative forcing by all  
165 aerosols produces a pronounced warming of 0.6 K/decade over the European Arctic, a

166 cooling of 0.6 K/decade over the Russian Arctic and a slight warming over the North  
167 American Arctic (Fig. 3a and b). The pattern of temperature trends in the all-aerosol case  
168 has elements in common with both sulfate-only and BC-only cases. In the sulfate-only  
169 experiment, there is a strong warming of 0.4 K/decade over the European and western  
170 Eurasian Arctic (Fig. 3c and d) where sulfate optical depth has declined (Fig. 1a). In and  
171 downstream of Siberia and in the western U.S. there is a significant cooling, which is  
172 contrary to what might be expected, given that sulfate concentrations and sulfate optical  
173 depth decreased across this region (Fig. 1). Such mismatch in the sign of temperature  
174 response and aerosol forcing is not unique to SO<sub>4</sub>. In BC-only simulations (Fig. 3e and  
175 3f), surface air temperatures warm 0.2 K/decade over the European Arctic, presumably in  
176 response to a reduction in BC concentrations aloft. There is a pronounced warming of  
177 roughly 0.4 K/decade over the Siberian and Alaskan Arctic and a strong cooling over the  
178 far north Atlantic despite small increases in BC optical depth in these regions. While  
179 there is some correspondence between the change in aerosol optical depths (Fig.1) and  
180 surface air temperatures (Fig. 3), the two are not perfectly correlated. This is because, in  
181 addition to the direct impact of aerosols on radiative fluxes, there may be other climate  
182 responses to the forcings which themselves affect surface air temperatures. In some  
183 cases, quite long-range connections are possible. Previous studies [Shindell and Faluvegi,  
184 2009; Sand et al., 2013; Flanner, 2013] regarding the role of remote aerosols on Arctic  
185 temperatures show that an increase in BC concentrations at low latitudes causes a  
186 warming in the Arctic. Such remote influence is also shown by Teng et al. [2012] who  
187 found surface warming over the Siberian Arctic in response to increasing BC  
188 concentrations in Asia in CCSM4 (see their Figure 2). We emphasize that these results

189 are specific to CCSM4. As shown in Koch et al. [2009], general circulation models have  
190 great variability in simulating BC aerosols. Even when using a fixed set of emissions,  
191 different models will simulate different horizontal and vertical distributions of aerosols,  
192 as well as differences in total atmospheric burden. Therefore it is of great interest for  
193 future studies to examine the climate response of BC using different models.

194

### 195 **3.2. Interpreting the climate responses to forcing**

196 To further understand the temperature trends we analyzed sea level pressure, sea  
197 ice coverage, radiative flux changes at top of the atmosphere (TOA) due to changes in  
198 clouds and changes in NHT using the transient sulfate-only and BC-only runs as  
199 described in section 2. NHT is calculated following equation (1) in Sand et al. [2012]. In  
200 the sulfate-only experiment (Fig. 4a-d), there is a dipole in sea level pressure trends, i.e.  
201 in the eastern North Atlantic versus in the European and west Eurasian Arctic. This draws  
202 warmer air northward from lower latitudes, consistent with the strong warming trend  
203 found in the European Arctic. The significant sea ice loss over the Barents Sea amplifies  
204 the warming there. Surface cooling over most of the rest of the Arctic is consistent with  
205 cold-air advection from Siberia, amplified by sea ice gain on the Siberian shelf and into  
206 the Chukchi and Beaufort Sea. Net changes in cloud radiative fluxes at TOA, which are  
207 the summation of shortwave and longwave fluxes, have a similar pattern to the changes  
208 in sea ice coverage. These show a radiative cooling effect over the European Arctic and  
209 warming over Siberia. NHT enhances the warming over the Eurasian Arctic and the  
210 cooling over the Siberian and North American Arctic. These findings suggest that direct  
211 surface radiative cooling from sulfate aerosols is the possible trigger for the surface

212 cooling while the dynamical response of atmospheric circulation, sea ice, and clouds  
213 work together to reinforce such temperature trends. Cloud changes have a weaker  
214 influence than sea ice and NHT changes in terms of magnitudes of trends. Again, we  
215 emphasize that the cloud changes produced here are only due to a thermodynamic  
216 response to the aerosol direct radiative forcing. If cloud microphysical effects were  
217 included in the model runs cloud changes might have a much more significant impact on  
218 Arctic climate.

219         The dynamical responses of the atmosphere and sea ice are similarly important in  
220 the BC-only experiment (Fig. 4e-h). Sea ice coverage decreases near the Barents Sea and  
221 the eastern Siberia shelf, where surface air temperature increases. NHT has strong  
222 positive trends over the Eurasian and North American Arctic. Therefore, the responses in  
223 both sea ice and NHT to aerosol direct radiative forcing reinforce the surface air  
224 temperature changes. Trends in net cloud radiative fluxes are weak and do not show a  
225 clear pattern.

226

#### 227 **4. Summary and discussion**

228         We use fully coupled CCSM4 with CAM4 physics to investigate the Arctic and  
229 global climate response to the change in concentrations of all aerosols, sulfate aerosols  
230 only and BC only during the three decades from 1975 to 2005. Single-forcing transient  
231 simulations were performed in order to isolate the impacts of all aerosols, sulfate only  
232 and BC only. The surface air temperature response to all aerosols is dominated by  
233 changes in sulfate, while the effects of BC are apparently mostly offset by coincident  
234 trends in OC. Globally averaged, trends in all aerosols produce a cooling trend of 0.015

235 K/decade during the period of 1975-2005, with 0.02 K/decade cooling driven by changes  
236 in sulfate aerosols. Averaged across the whole Arctic, surface air temperature shows no  
237 significant trend. However, there are pronounced geographical variations in temperature  
238 trends. Over the European Arctic, aerosols induce about 0.6 K/decade warming, or about  
239 1.8 K warming over the 30-year period from 1975 to 2005. This warming is triggered by  
240 a reduction in sulfate and BC concentrations over that region and is maintained by sea ice  
241 loss and a strengthening in NHT. Changes in sulfate concentrations account for about two  
242 thirds of the warming and BC for the remaining one-third. A recent study by Cowtan and  
243 Way [2014] shows that global temperature rise of the past 15 years has been largely  
244 underestimated due to data gaps especially in the Arctic. Based on the simulations  
245 presented here, we believe that sulfate aerosol trends have played an important role in the  
246 Arctic warming and potentially have prevented the warming “hiatus” seen in global  
247 temperature trends [Trenberth and Fasullo, 2013] from being seen in the Arctic  
248 temperature trends. Over the Siberian and North American Arctic, surface air temperature  
249 is likely influenced by changes of aerosol optical depth over Asia. An increase in sulfate  
250 optical depth over Asia induces a large cooling while an increase in BC optical depth  
251 over Asia causes a significant warming, consistent with Shindell and Faluvegi [2009].  
252 Thus, full understanding of drivers of Arctic climate change require accounting for  
253 changes in all aerosol species – not just BC – and of the climate responses to both local  
254 and remote forcings.

255

256

257

258 **Acknowledgements**

259 This research used computing resources at the National Center for Atmospheric Research  
260 (NCAR). We acknowledge Julie Arblaster and Adrienne Middleton for providing the  
261 restart files and CMIP5 sulfate-only runs. We thank Loretta Mickley, Thomas breider,  
262 Daniel Jacob, Mark Flanner and two anonymous reviewers for helpful discussions. This  
263 study was supported by the National Science Foundation grant ARC-1049002.

264 **References**

- 265 Armour, K. C., C. M. Bitz, G. H. Roe: Time-Varying Climate Sensitivity from Regional  
266 Feedbacks, *J. Climate*, 26, 4518–4534, doi: [http://dx.doi.org/10.1175/JCLI-D-12-](http://dx.doi.org/10.1175/JCLI-D-12-00544.1)  
267 00544.1, 2013.
- 268 Bond, T. C., Bhardwaj, E., Dong, R., Jogani, R., Jung, S., Roden, C., Streets, D. G., and  
269 Trautmann, N. M.: Historical emissions of black and organic carbon aerosol from  
270 energy-related combustion, 1850-2000, *Global Biogeochem. Cy.*, 21, GB2018,  
271 doi:10.1029/2006GB002840, 2007.
- 272 Bond, T. C., Doherty, S. J., Fahey, D. W., Forster, P. M., Berntsen, T., DeAngelo, B. J.,  
273 Flanner, M. G., Ghan, S., Kärcher, B., Koch, D., Kinne, S., Kondo, Y., Quinn, P. K.,  
274 Sarofim, M. C., Schultz, M. G., Schulz, M., Venkataraman, C., Zhang, H., Zhang, S.,  
275 Bellouin, N., Guttikunda, S. K., Hopke, P. K., Jacobson, M. Z., Kaiser, J. W.,  
276 Klimont, Z., Lohmann, U., Schwarz, J. P., Shindell, D., Storelvmo, T., Warren, S. G.,  
277 and Zenderm C. S.: Bounding the role of black carbon in the climate system: a  
278 scientific assessment, *J. Geophys. Res.-Atmos.*, 118, 5380–5552,  
279 doi:10.1002/jgrd.50171, 2013.
- 280 Cowtan, K. and Way, R. G.: Coverage bias in the HadCRUT4 temperature series and its  
281 impact on recent temperature trends, *Q.J.R. Meteorol. Soc.* doi: 10.1002/qj.2297,  
282 2014.
- 283 Flanner, M. G.: Arctic climate sensitivity to local black carbon, *Geophys. Res.*, 118,  
284 1840–1851, doi:10.1002/jgrd.50176, 2013.
- 285 Fyfe, J. C. et al.: One hundred years of Arctic surface temperature variation due to  
286 anthropogenic influence. *Sci. Rep.* 3, 2645, doi:10.1038/srep02645, 2013.

287 Gent, P. R., Danabasoglu, G., Donner, L. J., Holland, M. M., Hunke, E. C., Jayne, S. R.,  
288 Lawrence, D. M., Neale, R. B., Rasch, P. J., Vertenstein, M., Worley, P. H., Yang, Z.-  
289 L., and Zhang, M.: The community climate system model version 4, *J. Climate*, 24,  
290 4973–4991, doi:10.1175/2011JCLI4083.1, 2011.

291 Hess, M., P. Koepke, and I. Schult, Optical properties of aerosols and clouds: the  
292 software package OPAC, *Bull. Am. Meteorol. Soc.*, 79, 831-844, 1998.

293 Holland, M. M. and Bitz, C. M.: Polar amplification of climate change in the coupled  
294 model intercomparison project, *Clim. Dynam.*, 21, 221–232, 2003.

295 Junker, C. and Liousse, C.: A global emission inventory of carbonaceous aerosol from  
296 historic records of fossil fuel and biofuel consumption for the period 1860-1997,  
297 *Atmos. Chem. Phys.*, 8, 1195-1207, doi:10.5194/acp-8-1195-2008, 2008.

298 Kettle, A. J., M. O. Andreae, D. Amouroux, and T. W. Andreae: A global database of sea  
299 surface dimethylsulfide (DMS) measurements and a procedure to predict sea surface  
300 DMs as a function of latitude, longitude, and month, *Glob. Biogeochem. Cycles*, 13,  
301 399-444, 1999.

302 Koch, D. and Hansen, J.: Distant origins of Arctic black carbon: a Goddard Institute for  
303 Space Studies model experiment, *J. Geophys. Res.*, 110, D04204,  
304 doi:10.1029/2004JD005296, 2005.

305 Koch, D., Menon, S., Genio, A. D., Ruedy, R., Alienov, I., and Schmidt, G. A.:  
306 Distinguishing aerosol impacts on climate over the past century, *J. Climate*, 22, 2659–  
307 2677, 2009.

308 Koch, D., Schulz, M., Kinne, S., McNaughton, C., Spackman, J. R., Balkanski, Y.,  
309 Bauer, S., Berntsen, T., Bond, T. C., Boucher, O., Chin, M., Clarke, A., De Luca, N.,

310 Dentener, F., Diehl, T., Dubovik, O., Easter, R., Fahey, D. W., Feichter, J.,  
311 Fillmore, D., Freitag, S., Ghan, S., Ginoux, P., Gong, S., Horowitz, L., Iversen, T.,  
312 Kirkevåg, A., Klimont, Z., Kondo, Y., Krol, M., Liu, X., Miller, R., Montanaro, V.,  
313 Moteki, N., Myhre, G., Penner, J. E., Perlwitz, J., Pitari, G., Reddy, S., Sahu, L.,  
314 Sakamoto, H., Schuster, G., Schwarz, J. P., Seland, Ø., Stier, P., Takegawa, N.,  
315 Takemura, T., Textor, C., van Aardenne, J. A., and Zhao, Y.: Evaluation of black  
316 carbon estimations in global aerosol models, *Atmos. Chem. Phys.*, 9, 9001-9026,  
317 doi:10.5194/acp-9-9001-2009, 2009.

318 Lamarque, J.-F., Bond, T. C., Eyring, V., Granier, C., Heil, A., Klimont, Z., Lee, D.,  
319 Liousse, C., Mieville, A., Owen, B., Schultz, M. G., Shindell, D., Smith, S. J.,  
320 Stehfest, E., Van Aardenne, J., Cooper, O. R., Kainuma, M., Mahowald, N.,  
321 McConnell, J. R., Naik, V., Riahi, K., and van Vuuren, D. P.: Historical (1850–2000)  
322 gridded anthropogenic and biomass burning emissions of reactive gases and aerosols:  
323 methodology and application, *Atmos. Chem. Phys.*, 10, 7017-7039, doi:10.5194/acp-  
324 10-7017-2010, 2010.

325 Lamarque, J.-F., Kyle, G. P., Meinshausen, M., Riahi, K., Smith, S. J., van Vuuren, D. P.,  
326 Conley, A., and Vitt, F.: Global and regional evolution of short-lived radiatively-  
327 active gases and aerosols in the representative concentration pathways, *Climatic*  
328 *Change*, 109, 191–912, doi:10.1007/s10584-011-0155-0, 2011.

329 Lamarque, J.-F., Emmons, L. K., Hess, P. G., Kinnison, D. E., Tilmes, S., Vitt, F.,  
330 Heald, C. L., Holland, E. A., Lauritzen, P. H., Neu, J., Orlando, J. J., Rasch, P. J., and  
331 Tyndall, G. K.: CAM-chem: description and evaluation of interactive atmospheric  
332 chemistry in the Community Earth System Model, *Geosci. Model Dev.*, 5, 369-411,

333 doi:10.5194/gmd-5-369-2012, 2012.

334 IPCC: Climate Change 2007: The Physical Science Basis. Contribution of Working  
335 Group I to the Fourth Assessment Report of the Intergovernmental Panel on Climate  
336 Change, edited by: Solomon, S., Qin, D., Manning, M., Chen, Z., Marquis, M.,  
337 Averyt, K. B., Tignor, M., and Miller, H. L., Cambridge University Press, Cambridge,  
338 UK and New York, NY, USA, 2007.

339 Manabe, S. and Stouffer, R. J.: Sensitivity of a global climate model to an increase of  
340 CO<sub>2</sub> concentration in the atmosphere, *J. Geophys. Res.*, 85, 5529–5554, 1980.

341 Meehl, G. A., Washington, W. M., Arblaster, J. M., Hu, A., Teng, H., Tebaldi, C.,  
342 Sanderson, B. N., Lamarque, J.-F., Conley, A., Strand, W. G., and White III, J. B.:  
343 Climate system response to external forcings and climate change projections in  
344 CCSM4, *J. Climate*, 25, 3661–3683, 2012.

345 Neale, R. B., Richter, J. H., Conley, A. J., Park, S., Lauritzen, P. H., Gettelman, A.,  
346 Williamson, D. L., Rasch, P. J., Vavrus, S. J., Taylor, M. A., Collins, W. D., Zhang,  
347 M., and Lin, S.-J.: Description of the NCAR Community Atmosphere Model  
348 (CAM4), NCAR Tech. Rep. NCAR/TN-485+ STR, 212 pp., available at:  
349 [https://www.cesm.ucar.edu/models/ccsm4.0/cam/docs/description/cam4\\_desc.pdf](https://www.cesm.ucar.edu/models/ccsm4.0/cam/docs/description/cam4_desc.pdf),  
350 2011.

351 Pithan, F., T. Mauritsen: Comments on “Current GCMs' Unrealistic Negative Feedback  
352 in the Arctic”, *J. Climate*, 26, 7783–7788, doi: [http://dx.doi.org/10.1175/JCLI-D-12-](http://dx.doi.org/10.1175/JCLI-D-12-00331.1)  
353 00331.1, 2013.

354 Quinn, P. K., Bates, T. S., Baum, E., Doubleday, N., Fiore, A. M., Flanner, M., Fridlind,  
355 A., Garrett, T. J., Koch, D., Menon, S., Shindell, D., Stohl, A., and Warren, S. G.:

356 Short-lived pollutants in the Arctic: their climate impact and possible mitigation  
357 strategies, *Atmos. Chem. Phys.*, 8, 1723–1735, doi:10.5194/acp-8-1723-2008, 2008.

358 Sand, M., Berntsen, T. K., Kay, J. E., Lamarque, J. F., Seland, Ø., and Kirkevåg, A.: The  
359 Arctic response to remote and local forcing of black carbon, *Atmos. Chem. Phys.*, 13,  
360 211–224, doi:10.5194/acp-13-211-2013, 2013.

361 Screen, J. A. and Simmonds, I.: The central role of diminishing sea ice in recent Arctic  
362 temperature amplification, *Nature*, 464, 1334–1337, 2010.

363 Serreze, M. C. and Barry, R. G.: Processes and impacts of Arctic amplification: a  
364 research synthesis, *Global Planet. Change*, 77, 85–96,  
365 doi:10.1016/j.gloplacha.2011.03.004, 2011.

366 Serreze, M. C., Barrett, A. P., Stroeve, J. C., Kindig, D. N., and Holland, M. M.: The  
367 emergence of surface-based Arctic amplification, *The Cryosphere*, 3, 11–19,  
368 doi:10.5194/tc-3-11-2009, 2009.

369 Shindell, D. and Faluvegi, G.: Climate response to regional radiative forcing during the  
370 twentieth century, *Nat. Geosci.*, 2, 294–300, doi:10.1038/ngeo473, 2009.

371 Shindell, D. T., Lamarque, J.-F., Schulz, M., Flanner, M., Jiao, C., Chin, M., Young, P.  
372 J., Lee, Y. H., Rotstayn, L., Mahowald, N., Milly, G., Faluvegi, G., Balkanski, Y.,  
373 Collins, W. J., Conley, A. J., Dalsoren, S., Easter, R., Ghan, S., Horowitz, L., Liu, X.,  
374 Myhre, G., Nagashima, T., Naik, V., Rumbold, S. T., Skeie, R., Sudo, K., Szopa, S.,  
375 Takemura, T., Voulgarakis, A., Yoon, J.-H., and Lo, F.: Radiative forcing in the  
376 ACCMIP historical and future climate simulations, *Atmos. Chem. Phys.*, 13, 2939–  
377 2974, doi:10.5194/acp-13-2939-2013, 2013.

378 Smith, S. J., Steven, J., Pitcher, H., and Wigley, T. M. L.: Global and regional

379 anthropogenic sulfur dioxide emissions, *Global Planet. Change*, 29(1-2), 99-119,  
380 2001.

381 Smith, S. J., Andres, R., Conception, E., and Lurz, J.: Historical sulfur dioxide emissions  
382 1850-2000: Methods and results, PNNL Research Report, Joint Global Change  
383 Research Institute, 8400 Baltimore Avenue College Park, Maryland, 20740, 2004.

384 Taylor, K. E., Stouffer, R. J., and Meehl, G. A.: An overview of CMIP5 and the  
385 experiment design, *B. Am. Meteorol. Soc.*, 93, 485–498, doi:10.1175/BAMS-D-11-  
386 00094.1, 2012.

387 Teng, H., Washington, W. M., Branstator, G., Meehl, G. A., and Lamarque, J.-F.:  
388 Potential impacts of Asian carbon aerosols on future US warming, *Geophys. Res. Lett.*,  
389 39, L11703, doi:10.1029/2012GL051723, 2012.

390 Trenberth, K. E., and J. T. Fasullo: An apparent hiatus in global warming? *Earth's*  
391 *Future*, 1, 19–32, doi:10.1002/2013EF000165, 2013.

392 Twomey, S. A., M. Piepgrass, and T. L. Wolfe, An assessment of the impact of pollution  
393 on global cloud albedo, *Tellus*, 36, 356-366, 1984.

394

395

396

397

398

399

400

401

402

403

404

405 **Table 1.** List of experiments, number of ensemble members, whether the run was  
406 obtained from CMIP5 or it is a new run conducted in this study, run period, trend analysis  
407 period and aerosols that vary in the run.

Model experiment	# of ensemble members	CMIP5 or new run	Run period	Trend analysis Period	Aerosols that vary
All aerosols	3	CMIP5	1850 -- 2005	1975 -- 2005	SO <sub>4</sub> , BC and OC
SO <sub>4</sub> -only	3*	CMIP5	1850 -- 2005	1975 -- 2005	SO <sub>4</sub>
	6	New run	1920 -- 2005		
BC-only	6	New run	1920 -- 2005	1975 -- 2005	BC
Control	1	CMIP5	1850 -- 2005	N/A	None

408

409 \* only surface air temperature field was available.

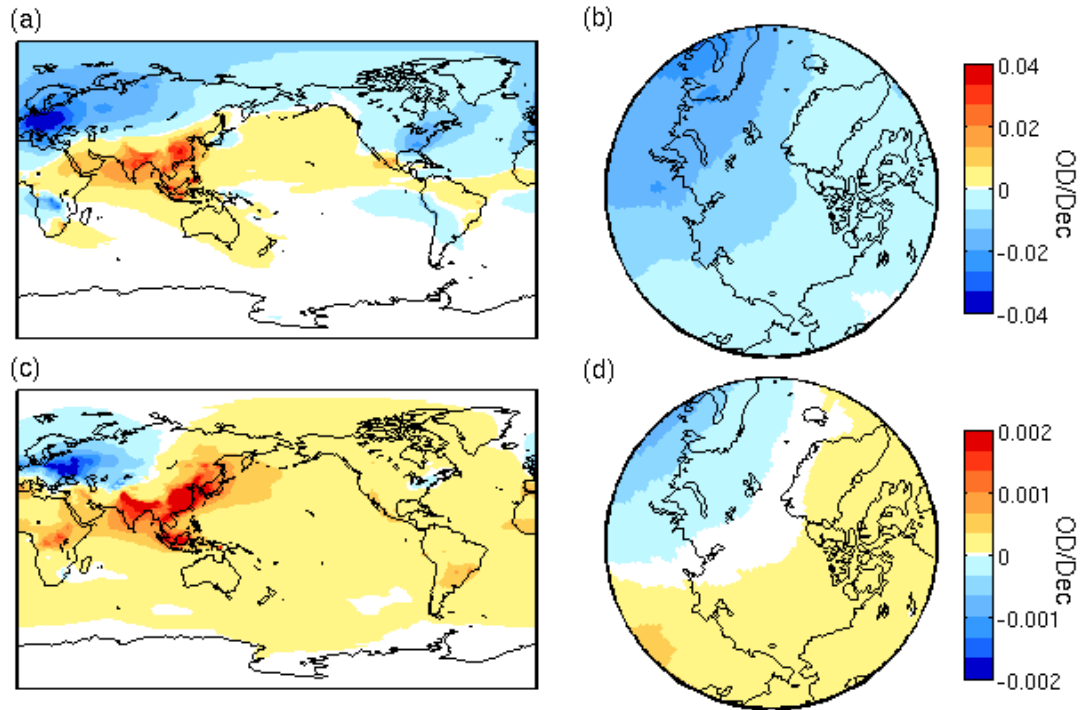
410

411

412

413

414

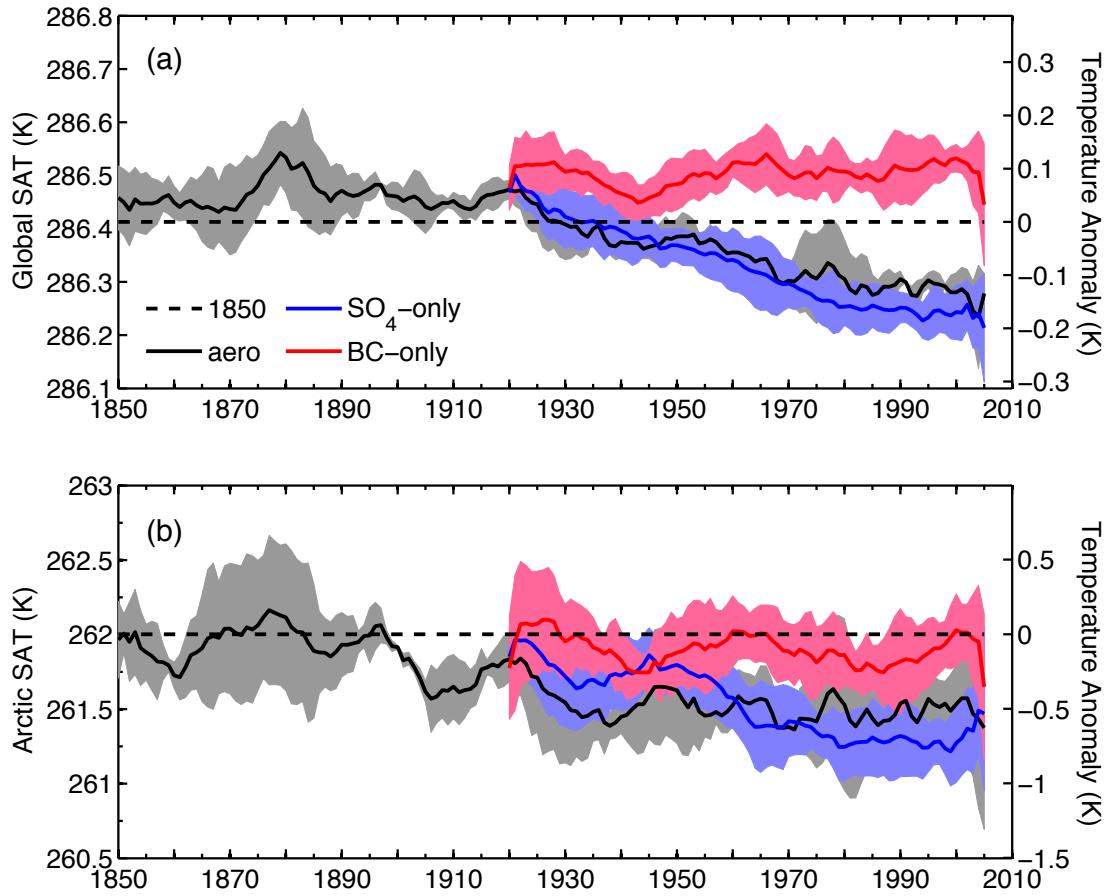


415

416 **Figure 1.** Linear trends in optical depths per decade for sulfate (a, b) and black carbon (c,

417 d) for the period 1975-2005, both globally and for the Arctic.

418



419

420 **Figure 2.** Time series of area-weighted, annual-mean surface air temperature (SAT) over  
 421 the globe (a) and Arctic (b) for all aerosol forcing (black), sulfate-only forcing (blue) and  
 422 BC-only forcing (red). Shading indicates one standard deviation of ensemble members.  
 423 A 9-year running mean was applied. A year 1850 control run is shown in black dashed  
 424 line.

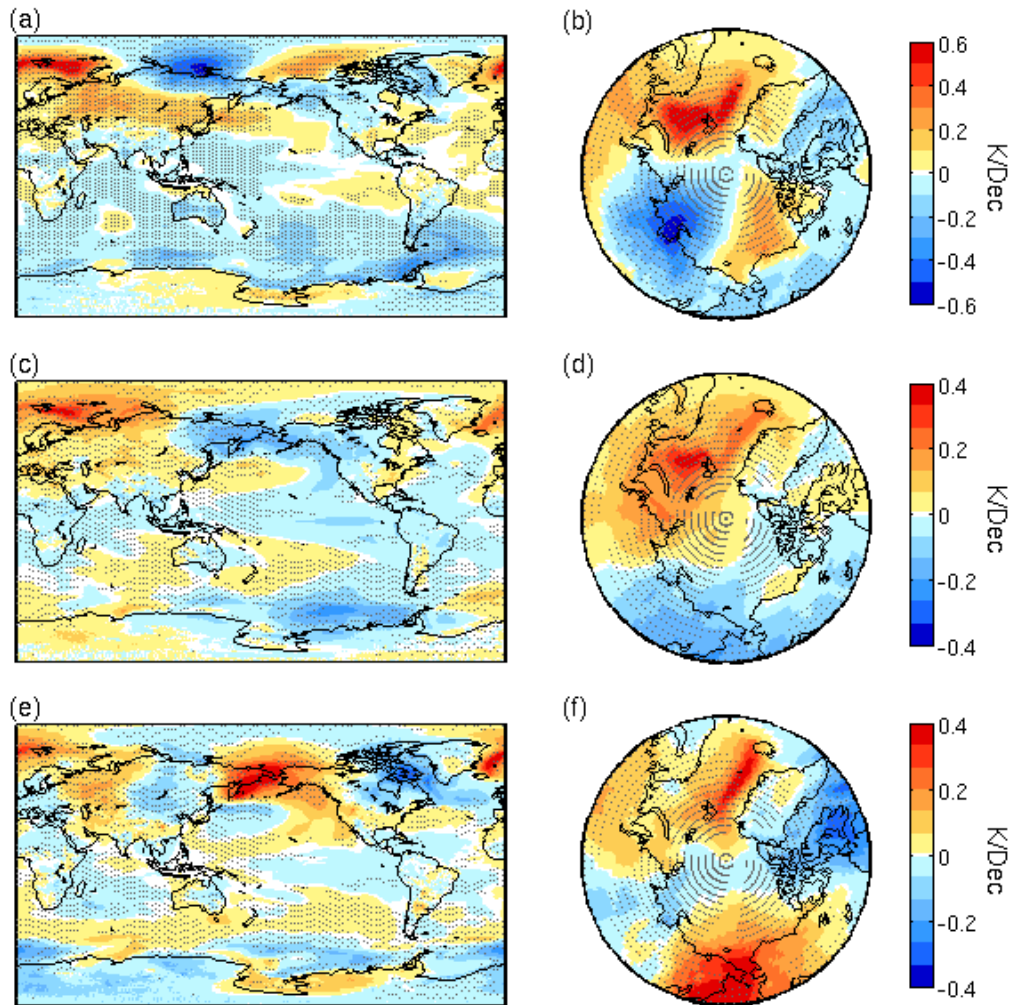
425

426

427

428

429



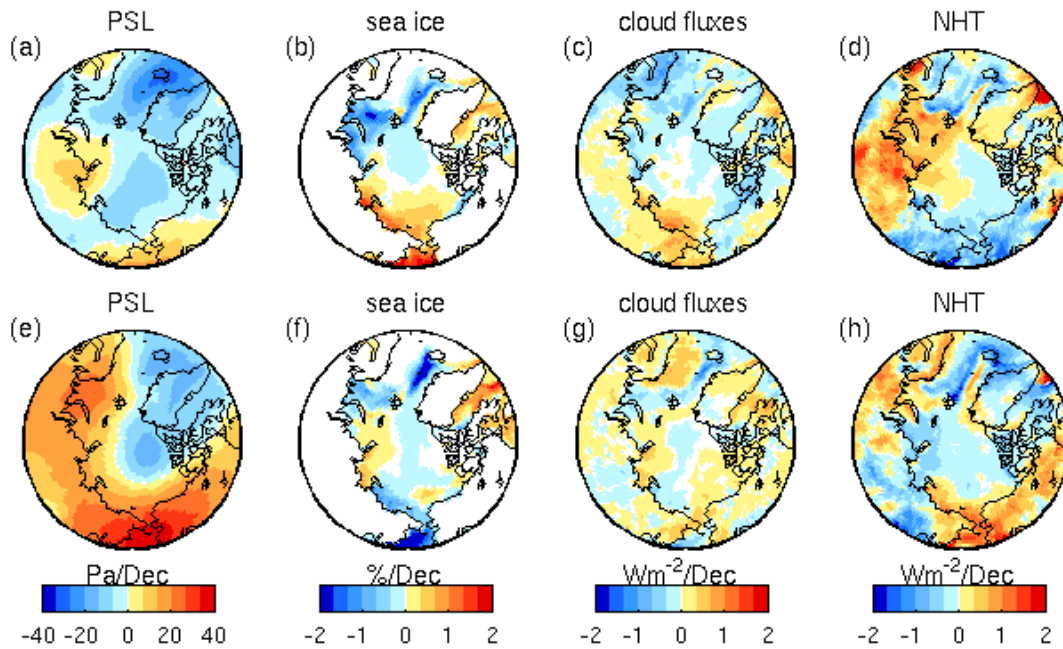
430

431 **Figure 3.** Linear trends in surface air temperature for the period 1975-2005 over the  
 432 globe and Arctic due to changes in all aerosols (a and b), sulfate only (c and d) and black  
 433 carbon only (e and f), respectively. Gray dots indicate trends that are statistically  
 434 significant at the 95% level ( $p < 0.05$ ) based on an F-test.

435

436

437



438

439 **Figure 4.** Linear trends in sea level pressure (PSL), sea ice coverage, cloud net radiative  
 440 fluxes at top of the atmosphere, and atmospheric northward heat transport (NHT) over the  
 441 period 1975-2005 in the Arctic due to direct radiative forcing by sulfate only (a, b, c and  
 442 d) and black carbon only (e, f, g and h), respectively.

443